Hindawi
Journal of Advanced Transportation
Volume 2022, Article ID 4092011, 13 pages
https://doi.org/10.1155/2022/4092011

Research Article

Synchronous Optimization for Demand-Driven Train Operation Plan in Rail Transit Network Using Nondominated Sorting Coevolutionary Memetic Algorithm

Zhenyu Han, Dewei Li, Baoming Han, and Han Gao

School of Traffic and Transportation, Beijing Jiaotong University, Beijing 100044, China

Correspondence should be addressed to Baoming Han; bmhan@bjtu.edu.cn

Received 22 April 2022; Revised 24 June 2022; Accepted 16 July 2022; Published 5 October 2022

Academic Editor: Zhihong Yao

In many cities and regions, decision makers independently develop Train Operation Plan (TOP) for each line in the rail transit network, resulting in a lack of TOP Synchronization (TOPS). Considering the entire network as a whole, researchers have realized that synchronous optimization is of great significance. In this paper, we formulate two Mixed-Integer Linear Programming (MILP) models to optimize demand-driven TOP in the network. The former is an Asynchronous TOP Optimization (ATOPO) model, while the latter is a Synchronous TOP Optimization (STOPO) model. The bi-objective models simultaneously determine train frequency, train timetable, and rolling stock circulation under small-granularity passenger demand to minimize trains' total cost and passengers' total time. Then, we propose the Nondominated Sorting Coevolutionary Memetic Algorithm (NSCMA) to solve the combinatorial optimization problems. The hybrid heuristic algorithm incorporates Coevolutionary Memetic Algorithm (CMA) into Advanced and Adaptive Nondominated Sorting Genetic Algorithm II (AANSGA-II) to ameliorate the evolution process for elite individuals. On this basis, we study the case of Shenyang Metro to verify the models and the algorithm. The results demonstrate that the STOPO model is better than the ATOPO model in reducing trains' total cost and passengers' total time. In addition, NSCMA is better than AANSGA-II in obtaining elite individuals.

1. Introduction

As carbon emissions become a global issue, governments have paid more and more attention to energy consumption [1]. In recent decades, rail transit has developed rapidly around the world as an environmentally friendly mode of public transport. The rail transit systems in many cities and regions have entered the network era. However, lines in most networks are connected only by transfer stations, and trains on most lines are organized independently.

Since researchers know the independence of lines, ATOPO has become a hot issue. In these problems, lines are separated from the network, and TOPs are separately optimized for each line. Several studies have made significant progresses on demand-driven ATOPO problems [2–11]. These studies considered nontransfer passengers but omitted transfer passengers. Therefore, the asynchronously optimized TOPs are probably optimal for nontransfer passengers but probably not optimal for transfer passengers.

Since researchers understand the importance of transfer passengers, TOPS has become another hot issue. In these problems, transfer stations are separated from the network, and TOPs are synchronized for the network. Several studies have made many contributions to TOPS problems. Wong et al. [12] combined a heuristic algorithm with CPLEX to solve a TOPS model aiming at minimizing passengers' transfer waiting time. Wu et al. [13] presented a TOPS model to minimize the maximal transfer waiting time while limiting passengers' transfer waiting time equitably over any transfer station. Guo et al. [14] constructed a TOPS model to maximize the number of transfer synchronization events for the transitional period (from peak to off-peak hours or vice versa). A hybrid heuristic algorithm combined particle swarm optimization with simulated annealing to obtain near-optimal solutions efficiently. Liu et al. [15] built a TOPS model for minimizing passengers' transfer waiting time. Tian and Niu [16] developed a TOPS model to minimize passengers' transfer waiting time and maximize the number

of connections. A novel sequential search algorithm solved the bi-objective model. Cao et al. [17] proposed a Genetic Algorithm (GA for short) with a Local Search (LS for short) strategy to solve a TOPS model by maximizing the number of connections. These studies considered transfer passengers but omitted nontransfer passengers. Therefore, the synchronized TOPs are probably optimal for transfer passengers but probably not optimal for nontransfer passengers.

Since researchers realize the importance of all passengers, STOPO has become an acknowledged challenge. STOPO overcomes the drawbacks of ATOPO and TOPS. In these problems, the network is seen as a whole, and TOPs are simultaneously optimized for the network. Several studies have made some attempts at STOPO problems. Niu et al. [18] presented a demand-driven STOPO model aimed at minimizing passengers' waiting time and crowding disutility. Robenek et al. [19] constructed a demand-driven STOPO model to maximize companies' profit and passengers' satisfaction. Shang et al. [20] built a demand-driven STOPO model for minimizing passengers' travel time. Wang et al. [21] developed a demand-driven STOPO model to minimize passengers' waiting time and the number of passengers with failed transfers. Han et al. [22] formulated a demand-driven STOPO model to minimize trains' operation cost and passengers' total time. AANSGA-II obtained an approximate Pareto Optimal Solution Set (POSS for short) efficiently. These studies considered train formation, train frequency, and train timetable but omitted rolling stock circulation. Therefore, the synchronously optimized TOPs lack practicality.

This paper focuses on an integrated demand-driven TOP Optimization (TOPO for short) problem in the rail transit network. Two bi-objective MILP models called the ATOPO model and the STOPO model simultaneously determine train frequency, train timetable, and rolling stock circulation under small-granularity passenger demand to minimize trains' total cost and passengers' total time. A hybrid heuristic algorithm called NSCMA efficiently solves the bi-objective problem by ameliorating the evolution process for elite individuals based on AANSGA-II. A case study of Shenyang Metro verifies that the STOPO model is better than the ATOPO model and that NSCMA is better than AANSGA-II.

This paper is organized as follows: Section 2 states the demand-driven TOPO problem. Section 3 formulates the ATOPO and STOPO models. Section 4 proposes NSCMA. Section 5 studies the case of Shenyang Metro. Section 6 presents the conclusions.

2. Problem Statement

We focus on a network formed by a set of bidirectional lines $S_l\{1, 2, \cdots, L\}$. Each line $l \in S_l$ contains a set of stations $S_i^l\{1, 2, \cdots, I_l, \cdots, 2I_l\}$ and a set of transfer stations $S_j^l\{1, 2, \cdots, J_l, \cdots, 2J_l\}$, as illustrated in Figure 1. Each physical station on line l refers to i_l and $2I_l + 1 - i_l$ in both directions, and each physical transfer station on line l refers to j_l and $2J_l + 1 - j_l$ in both directions.

We use station $i(j_l)$ to reindex transfer station j_l. Each transfer station $j_l \in S_j^l$ refers to station $i(j_l) \in S_i^l$. On this basis, the set of transfer stations $S_j^l\{1, 2, \cdots, J_l, \cdots, 2J_l\}$ corresponds to a set of stations $S_{li}^0\{i(1), i(2), \cdots, i(J_l), \cdots, i(2J_l)\}$. Binary parameter $q_{jj'}^{ll'}$ equals to one if transfer corridor $(j_l, j_{l'}')$ is valid.

We schedule a set of trains $S_k^l\{1, 2, \cdots, K_l^0, \cdots, K_l\}$ with capacity c_l on each line $l \in S_l$. Limited by the maximum transport capacity, at most K_l trains run on line l with headways of at least $h_{\min}^l$. Required by the minimum service level, at least K_l^0 trains run on line l with headways of at most $h_{\max}^l$. Each active train $k_l \in S_k^l$ on line l runs from station 1 to station $2I_l$. We preset dwell time d_j^l (at transfer station j_l), travel time e_i^l (from station 1 to station i_l), the earliest departure time $g_{\min}^{lk}$ and the latest departure time $g_{\max}^{lk}$ of each train, essential cycle time e_l^0 (on line l) of each connection as well as transfer walking time $f_{jj'}^{ll'}$ (in transfer corridor $(j_l, j_{l'}')$) of each transfer passenger.

Assumption 1. We assume that no line adopts overtaking, skip-stop, cross-line, multi-routing, and multi-marshalling strategies.

We construct a set of time slices $S_t^l\{T_l^0, T_l^0 + 1, \cdots, T_l\}$ (also known as a set of time points) with length τ to express the time period of line l. Combining the time periods of all lines, the time period of the network is expressed as $S_t\{T^0, T^0 + 1, \cdots, T\}$. Notably, the time periods of all stations on line l are normalized. The normalization of time periods reduces the dimension of variables effectively [22].

We describe dynamic passenger demand as small-granularity cumulative number of arriving passengers p_{it}^l (at station i_l at time t), alighting ratio of loaded passengers a_{it}^l (at station i_l at time t) and transferring ratio of alighting passengers $o_{jj't}^{ll'}$ (to transfer corridor $(j_l, j_{l'}')$ at time t). The data are processed from small-granularity origin-destination matrices for simplicity [22].

Assumption 2. We assume that passengers from the outside arrive evenly during each time slice.

We design three binary variables and three integer variables for the demand-driven TOPO problem, as represented in formulas (1)–(6). Binary variable x_{kt}^l equals to one if train k_l departs at time t. Binary variable $w_{kk'}^l$ equals to one if train k_l connects train k_l'. Binary variable $y_{jj'kt}^{ll'}$ equals to one if transfer passengers in transfer corridor $(j_l, j_{l'}')$ from train k_l arrive at time t. Integer variable u_{ik}^l indicates the number of loaded passengers on train k_l in section $(i_l, i_l + 1)$. Integer variable b_{it}^l denotes the number of boarding passengers at station i_l at time t. Integer variable $v_{jj't}^{ll'}$ represents the number of transfer passengers in transfer corridor $(j_l, j_{l'}')$ at time t.

$$x_{kt}^l \in \{0, 1\}, \forall l \in S_l, \forall k_l \in S_k^l, \forall t \in S_t^l, \tag{1}$$

$$w_{kk'}^l \in \{0, 1\}, \forall l \in S_l, \forall k_l \in S_k^l, \forall k_l' \in S_k^l, \tag{2}$$

$$\begin{aligned} &y_{jj'kt}^{ll'} \in \{0, 1\}, \forall l \in S_l, \forall l' \in S_l, \forall j_l \in S_j^l, \\ &\forall j_{l'}' \in S_j^{l'}, \forall k_l \in S_k^l, \forall t \in S_t, \end{aligned} \tag{3}$$

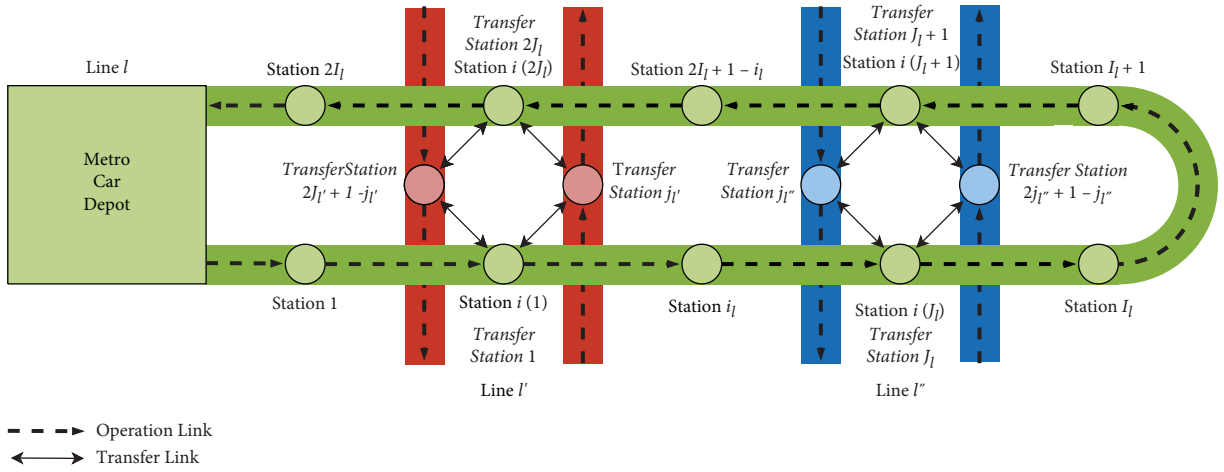

Figure 1: Sketch map of each line.

$$u_{ik}^{l} \in \mathrm{N}, \forall l \in S_l, \forall i_l \in S_i^l, \forall k_l \in S_k^l, \tag{4}$$

$$b_{it}^{l} \in \mathrm{N}, \forall l \in S_l, \forall i_l \in S_i^l, \forall t \in S_t^l, \tag{5}$$

$$v_{jj't}^{ll'} \in \mathrm{N}, \forall l \in S_l, \forall l' \in S_l, \forall j_l \in S_j^l, \forall j_{l'}' \in S_j^{l'}, \forall t \in S_t. \tag{6}$$

3. Mathematical Models

3.1. Asynchronous Train Operation Plan Optimization Model. The ATOPO model separately optimizes the TOP for each line in the network. It is formulated as a MILP model. Although binary variables are more than integer variables in formulating the same problem, the MILP model is linear without processing [23].

3.1.1. Objective Function. The ATOPO model aims to minimize generalized cost Z_l of line l for companies and passengers in (7). On the one hand, we select trains' total cost Z_{TTC}^l to express companies' cost of line l. On the other hand, we select passengers' total time Z_{PTT}^l under weight μ to represent passengers' cost of line l.

$$\min Z_l = Z_{TTC}^l + \mu * Z_{PTT}^l, \forall l \in S_l. \tag{7}$$

Trains' total cost Z_{TTC}^l of line l includes trains' operation cost Z_{TOC}^l and trains' depreciation cost Z_{TDC}^l, as represented in (8).

$$Z_{TTC}^l = Z_{TOC}^l + Z_{TDC}^l, \forall l \in S_l. \tag{8}$$

Trains' operation cost Z_{TOC}^l of line l equals to unit operation cost m_l multiplied by the number of trains, as shown in (9). The number of trains on line l is accumulated by binary variable x_{kt}^l.

$$Z_{TOC}^l = \sum_{k_l \in S_k^l} \sum_{t \in S_t^l} m_l * x_{kt}^l, \forall l \in S_l. \tag{9}$$

Trains' depreciation cost Z_{TDC}^l of line l equals to unit depreciation cost m_l^0 multiplied by the number of rolling stocks, as displayed in (10). The number of rolling stocks on line l equals to the number of trains minus the number of connections. The number of connections on line l is accumulated by binary variable $w_{kk'}^l$.

$$Z_{TDC}^l = \sum_{k_l \in S_k^l} \sum_{t \in S_t^l} m_l^0 * x_{kt}^l - \sum_{k_l \in S_k^l} \sum_{k_l' \in S_k^l} m_l^0 * w_{kk'}^l, \forall l \in S_l. \tag{10}$$

Passengers' total time Z_{PTT}^l of line l includes passengers' waiting time Z_{PWT}^l and passengers' penalty time Z_{PPT}^l, as represented in (11).

$$Z_{PTT}^l = Z_{PWT}^l + Z_{PPT}^l, \forall l \in S_l. \tag{11}$$

Passengers' waiting time Z_{PWT}^l of line l consists of passengers' basic waiting time and passengers' additional waiting time, as shown in (12). Passengers' basic waiting time of line l equals to half τ multiplied by the number of arriving passengers from the outside. Passengers' additional waiting time of line l equals to τ multiplied by the number of waiting passengers.

$$Z_{PWT}^l = \tau * \left(\frac{1}{2} \sum_{i_l \in S_i^l} p_{iT}^l + \sum_{i_l \in S_i^l} \sum_{t=T_l^0}^{T_l - 1} p_{it}^l - \sum_{i_l \in S_i^l} \sum_{t=T_l^0}^{T_l - 1} \sum_{t'=T_l^0}^{t} b_{it'}^l \right), \quad \forall l \in S_l. \tag{12}$$

Passengers' penalty time Z_{PPT}^l of line l equals to unit penalty time ε multiplied by the number of finally stranded passengers, as displayed in (13).

$$Z_{PPT}^l = \varepsilon * \left(\sum_{i_l \in S_i^l} p_{iT}^l - \sum_{i_l \in S_i^l} \sum_{t \in S_t^l} b_{it}^l \right), \forall l \in S_l. \tag{13}$$

3.1.2. Constraints. The ATOPO model is subject to train constraints, connection constraints, and passenger constraints.

(1) Train Constraints. Train constraints stipulate the uniqueness, priority, departure time, and headway of each train, as well as the number of trains.

Constraints (14) and (15) specify the uniqueness of each train. Each time point can only correspond to at most one active train. Meanwhile, each train can only correspond to at most one time point.

$$\sum_{k_l \in S_k^l} x_{kt}^l \le 1, \forall l \in S_l, \forall t \in S_t^l, \tag{14}$$

$$\sum_{t \in S_t^l} x_{kt}^l \le 1, \forall l \in S_l, \forall k_l \in S_k^l. \tag{15}$$

Constraint (16) states the priority of each train. A train should be inactive if the previous train is inactive.

$$\sum_{t \in S_t^l} x_{kt}^l \le \sum_{t \in S_t^l} x_{k-1,t}^l, \forall l \in S_l, \forall k_l \in \left(S_k^l \backslash \{1\}\right). \tag{16}$$

Constraints (17) and (18) limit that the departure time of each active train should be between $g_{\min}^{lk}$ and $g_{\max}^{lk}$.

$$\sum_{t \in S_t^l} t * x_{kt}^l \ge \frac{g_{\min}^{lk}}{\tau} * \sum_{t \in S_t^l} x_{kt}^l, \forall l \in S_l, \forall k_l \in S_k^l, \tag{17}$$

$$\sum_{t \in S_t^l} t * x_{kt}^l \le \frac{g_{\max}^{lk}}{\tau} * \sum_{t \in S_t^l} x_{kt}^l, \forall l \in S_l, \forall k_l \in S_k^l. \tag{18}$$

Constraints (19) and (20) limit that the headway of each active train should be between h_{min}^l and h_{max}^l.

$$\sum_{t \in S_t^l} t * x_{kt}^l - \sum_{t \in S_t^l} t * x_{k-1,t}^l \ge \frac{h_{\min}^l}{\tau} - 2T_l * \left(1 - \sum_{t \in S_t^l} x_{kt}^l\right), \forall l \in S_l, \forall k_l \in \left(S_k^l \backslash \{1\}\right), \tag{19}$$

$$\sum_{t \in S_t^l} t * x_{kt}^l - \sum_{t \in S_t^l} t * x_{k-1,t}^l \le \frac{h_{\max}^l}{\tau} + 2T_l * \left(1 - \sum_{t \in S_t^l} x_{kt}^l\right), \forall l \in S_l, \forall k_l \in \left(S_k^l \backslash \{1\}\right). \tag{20}$$

Constraints (21) and (22) limit that the number of trains should be between K_l^0 and K_l.

$$\sum_{k_l \in S_k^l} \sum_{t \in S_t^l} x_{kt}^l \ge K_l^0, \forall l \in S_l, \tag{21}$$

$$\sum_{k_l \in S_k^l} \sum_{t \in S_t^l} x_{kt}^l \le K_l, \forall l \in S_l. \tag{22}$$

(2) Connection Constraints. Connection constraints stipulate the uniqueness and cycle time of each connection.

Constraints (23) and (24) clarify the uniqueness of each connection. Each active train can only connect at most one active train. Meanwhile, each active train can only be connected by at most one active train.

$$\sum_{k_l' \in S_k^l} w_{kk'}^l \le \sum_{t \in S_t^l} x_{kt}^l, \forall l \in S_l, \forall k_l \in S_k^l, \tag{23}$$

$$\sum_{k_l' \in S_k^l} w_{k'k}^l \le \sum_{t \in S_t^l} x_{kt}^l, \forall l \in S_l, \forall k_l \in S_k^l. \tag{24}$$

Constraint (25) claims that the cycle time of each connection should be at least e_l^0.

$$\sum_{t \in S_t^l} t * x_{kt}^l - \sum_{t \in S_t^l} t * x_{k't}^l \ge \frac{e_l^0}{\tau} - 2T_l * \left(1 - w_{kk'}^l\right), \quad \forall l \in S_l, \forall k_l \in S_k^l, \forall k_l' \in S_k^l. \tag{25}$$

(3) Passenger Constraints. Passenger constraints stipulate the number of loaded and boarding passengers.

Constraint (26) limits that the number of loaded passengers should not exceed c_l if the train is active and equals to zero otherwise.

$$u_{ik}^l \le c_l * \sum_{t \in S_t^l} x_{kt}^l, \forall l \in S_l, \forall i_l \in S_i^l, \forall k_l \in S_k^l. \tag{26}$$

Constraint (27) limits that the number of boarding passengers should not exceed c_l if an active train departs at the time point and equals to zero otherwise.

$$b_{it}^l \le c_l * \sum_{k_l \in S_k^l} x_{kt}^l, \forall l \in S_l, \forall i_l \in S_i^l, \forall t \in S_t^l. \tag{27}$$

Constraints (28)–(31) declare the quantitative relationship between loaded passengers and boarding passengers. Constraints (28) and (29) are only for station 1, while Constraints (30) and (31) are only for the other stations. The number of loaded passengers should correspond to the number of boarding passengers and the number of alighting passengers. The number of alighting passengers should be equal to the alighting ratio multiplied by the number of loaded passengers.

$$u_{1k}^l \ge b_{1t}^l - c_l * \left(1 - x_{kt}^l\right), \forall l \in S_l, \forall k_l \in S_i^l, \forall t \in S_t^l, \tag{28}$$

$$u_{1k}^l \le b_{1t}^l + c_l * \left(1 - x_{kt}^l\right), \forall l \in S_l, \forall k_l \in S_i^l, \forall t \in S_t^l, \tag{29}$$

$$u_{ik}^{l} \geq b_{it}^{l} + u_{i-1,k}^{l} * \left(1 - a_{it}^{l}\right) - c_l * \left(1 - x_{kt}^{l}\right), \quad \forall l \in S_l, \forall i_l \in \left(S_k^l \backslash \{1\}\right), \forall k_l \in S_k^l, \forall t \in S_t^l, \tag{30}$$

$$u_{ik}^{l} \leq b_{it}^{l} + u_{i-1,k}^{l} * \left(1 - a_{it}^{l}\right) + c_l * \left(1 - x_{kt}^{l}\right), \quad \forall l \in S_l, \forall i_l \in \left(S_k^l \backslash \{1\}\right), \forall k_l \in S_k^l, \forall t \in S_t^l. \tag{31}$$

Constraint (32) specifies the quantitative relationship between boarding passengers and arriving passengers. The cumulative number of boarding passengers should not exceed the cumulative number of arriving passengers.

$$\sum_{t'=T_l^0}^{t} b_{it'}^{l} \leq p_{it}^{l}, \forall l \in S_l, \forall i_l \in S_i^l, \forall t \in S_t^l. \tag{32}$$

In summary, the ATOPO model consists of the objective function and constraints as follows:

$$\text{ATOPO model} \begin{cases} \text{Objective function: (7) – (13);} \\ \text{Train constraints: (14) – (22);} \\ \text{Connection constraints: (23) – (25);} \\ \text{Passenger constraints: (26) – (32);} \\ \text{Variable definitions: (1) – (2), (4) – (5).} \end{cases} \tag{33}$$

3.2. Synchronous Train Operation Plan Optimization Model. The STOPO model simultaneously optimizes the TOPs for all lines in the network. It is also formulated as a MILP model.

3.2.1. Objective Function. The STOPO model aims to minimize generalized cost Z of the network in (34).

$$\min Z = Z_{TTC} + \mu * Z_{PTT}. \tag{34}$$

Trains' total cost Z_{TTC} of the network includes trains' operation cost Z_{TOC} and trains' depreciation cost Z_{TDC}, which are accumulated by trains' operation cost Z_{TOC}^{l} and trains' depreciation cost Z_{TDC}^{l} of each line, respectively, as represented in (35)-(37).

$$Z_{TTC} = Z_{TOC} + Z_{TDC}, \tag{35}$$

$$Z_{TOC} = \sum_{l \in S_l} Z_{TOC}^{l}, \tag{36}$$

$$Z_{TDC} = \sum_{l \in S_l} Z_{TDC}^{l}. \tag{37}$$

Passengers' total time Z_{PTT} of the network includes passengers' waiting time Z_{PWT} and passengers' penalty time Z_{PPT}, which are accumulated by passengers' waiting time Z_{PWT}^{l} and passengers' penalty time Z_{PPT}^{l} of each line, respectively, as represented in (38)–(40). Since arriving passengers from the transfer corridors also wait for trains, passengers' waiting time Z_{PWT} and passengers' penalty time Z_{PPT} should also consider arriving passengers from the transfer corridors.

$$Z_{PTT} = Z_{PWT} + Z_{PPT}, \tag{38}$$

$$Z_{PWT} = \sum_{l \in S_l} Z_{PWT}^{l} + \tau * \sum_{l \in S_l} \sum_{l' \in S_l} \sum_{j_l \in S_j^l} \sum_{j_{l'} \in S_j^{l'}} \sum_{t=T_l^0}^{T_l - 1} \sum_{t'=T_l^0}^{t} v_{jj't}^{ll'}, \tag{39}$$

$$Z_{PPT} = \sum_{l \in S_l} Z_{PPT}^{l} + \varepsilon * \sum_{l \in S_l} \sum_{l' \in S_l} \sum_{j_l \in S_j^l} \sum_{j_{l'} \in S_j^{l'}} \sum_{t \in S_t^l} v_{jj't}^{ll'}. \tag{40}$$

3.2.2. Constraints. The STOPO model not only inherits all the constraints in the ATOPO model but also supplements several new constraints.

Constraints (41) and (42) declare the quantitative relationship between boarding passengers and arriving passengers to replace constraint (32). Constraint (41) is only for the nontransfer stations, while constraint (42) is only for the transfer stations.

$$\sum_{t'=T_l^0}^{t} b_{it'}{}^{l} \leq p_{it}^{l}, \forall l \in S_l, \forall i_l \in \left(S_i^l \backslash S_{li}^0\right), \forall t \in S_t^l, \tag{41}$$

$$\sum_{t'=T_l^0}^{t} b_{i(j)t'}{}^{l} \leq p_{i(j)t}^{l} + \sum_{l' \in S_l} \sum_{j_{l'} \in S_j^l} \sum_{t'=T_l^0}^{t} v_{jjt}^{ll'}, \forall l \in S_l, \forall j_l \in S_j^l, \forall t \in S_t^l. \tag{42}$$

In addition, passenger constraints also stipulate the uniqueness and arriving time of each transfer passenger, and the number of transfer passengers.

Constraint (43) states the uniqueness of each transfer passenger. Each transfer passenger should alight from an active train, walk in a valid transfer corridor, and arrive at a time point.

$$\sum_{t \in S_t} y_{jj'kt}^{ll'} = q_{jj'}^{ll'} * \sum_{t \in S_t^l} x_{kt}^{l}, \forall l \in S_l, \forall l' \in S_l, \forall j_l \in S_j^l, \forall j_{l'} \in S_j^{l'}, \forall k_l \in S_k^l. \tag{43}$$

Constraint (44) clarifies that the arrival time of each transfer passenger should correspond to the departure time of the train from which the transfer passenger alights.

$$\sum_{t\in S_t} t * y_{jj'kt}^{ll'} = q_{jj'}^{ll'} * \left(\sum_{t\in S_t^l} t * x_{kt}^l + \frac{\left(e_{i(j)}^l - e_{i(j')}^{l'} + f_{j'j}^{ll'} - d_j^l\right)}{\tau} * \sum_{t\in S_t^l} x_{kt}^l \right), \tag{44}$$

$$\forall l \in S_l, \forall l' \in S_l, \forall j_l \in S_j^l, \forall j_{l'}' \in S_j^{l'}, \forall k_l \in S_k^l.$$

Constraint (45) limits that the number of transfer passengers should not exceed c_l if an active train departs at the time point and equals to zero otherwise.

$$v_{jj't}^{ll'} \le c_l * q_{jj'}^{ll'} * \sum_{k_l\in S_k^l} y_{jj'kt}^{ll'}, \forall l \in S_l, \forall l' \in S_l, \forall j_l \in S_j^l, \forall j_{l'}' \in S_j^{l'}, \forall l \in S_t. \tag{45}$$

Constraints (46) and (47) claim the quantitative relationship between transfer passengers and loaded passengers. The number of transfer passengers should be equal to the transferring ratio multiplied by the number of alighting passengers.

$$v_{jj't}^{ll'} \ge u_{i(j)-1,k}^l * a_{i(j)t}^l * o_{jj't}^{ll'} - c_l * \left(1 - y_{jj'kt}^{ll'}\right), \forall l \in S_l, \forall l' \in S_l, \forall j_l \in S_j^l, \forall j_{l'}' \in S_j^{l'}, \forall k_l \in S_k^l,$$

$$\forall t \in S_t^l, \forall t' \in S_t,\ t' = t + \frac{\left(e_{i(j)}^l - e_{i(j')}^{l'} + f_{j'j}^{ll'} - d_j^l\right)}{\tau}, \tag{46}$$

$$v_{jj't}^{ll'} \le u_{i(j)-1,k}^l * a_{i(j)t}^l * o_{jj't}^{ll'} + c_l * \left(1 - y_{jj'kt}^{ll'}\right), \forall l \in S_l, \forall l' \in S_l, \forall j_l \in S_j^l, \forall j_{l'}' \in S_j^{l'}, \forall k_l \in S_k^l, \forall t \in S_t^l, \forall t' \in S_t,\ t'$$

$$= t + \frac{\left(e_{i(j)}^l - e_{i(j')}^{l'} + f_{j'j}^{ll'} - d_j^l\right)}{\tau}. \tag{47}$$

In summary, the STOPO model consists of the objective function and constraints as follows:

$$\text{STOPOmodel} \begin{cases} \text{Objective function: (9) – (10), (12) – (13), (34) – (40);} \\ \text{Train constraints: (14) – (22);} \\ \text{Connection constraints: (23) – (25);} \\ \text{Passenger constraints: (26) – (31), (41) – (47);} \\ \text{Variable definitions: (1) – (6).} \end{cases} . \tag{48}$$

4. Nondominated Sorting Coevolutionary Memetic Algorithm

4.1. Algorithm Scheme. With the progress in artificial intelligence, machine learning algorithms have been widely used in transportation research [24–26]. However, heuristic algorithms are still the most common method to solve TOPO problems as they have been proven to be NP-hard problems [27].

The demand-driven TOPO models in this paper aim to minimize generalized cost for companies and passengers, in which weight μ is undetermined. Since decision makers expect different μ in different situations, a novel heuristic algorithm that can obtain an approximate POSS is appropriate. We select AANSGA-II to build the algorithm scheme.

AANSGA-II originates from NSGA-II. NSGA-II is a classical heuristic algorithm for solving multi-objective problems [28]. AANSGA-II improves NSGA-II in three

aspects for TOPO problems. In local sorting, AANSGA-II proposes neighborhood distance instead of crowding distance to sequence the individuals in each frontier appropriately. In crossover and mutation, AANSGA-II introduces a scoring mechanism and alternative operators to produce the offspring population effectively. In population initialization, AANSGA-II adopts boundary individuals to generate the initial population reasonably. [22].

Despite these improvements, AANSGA-II also shows a drawback. Due to the nature of local sorting, AANSGA-II tends to pursue the first frontier rather than the elite individuals. We select CMA to improve the algorithm mechanism.

CMA originates from MA. MA combines GA with LS to improve computation efficiency and solution quality. Excellent individuals generated by LS participate in GA instead of original individuals [29, 30]. CMA improves MA by encoding LS settings (i.e., position, direction, step, strategy, and other parameters) as memes for coevolution [31, 32].

Inspired by MA based on NSGA-II, NSCMA incorporates CMA into AANSGA-II [33, 34]. It consists of population initialization, local search, nondominated sorting, local sorting, tournament selection, crossover and mutation, population combination, population replacement, POSS extraction, operator scoring, and termination judgement, as demonstrated in Table 1.

Table 1: Pseudo code of NSCMA.

	Nondominated sorting coevolutionary memetic algorithm
1	**Start**
2	Number of generations for final termination: Λ;
3	Number of generations for early termination: Λ';
4	Number of generations for operator scoring: Λ^0;
5	Size of population: Θ;
6	Representative weights of passengers' total time: μ;
7	Probabilities of operators: P, P_π, $P_{\bar{\omega}}$;
8	Tolerance factor of reference point: γ;
9	Objective values of benchmark individual: Z^0_{TTC}, Z^0_{PTT};
10	Index of current generation: $\lambda \leftarrow 1$;
11	$S_{\text{parent}} \leftarrow$ **Population initialization** ();
12	$S_{\text{parent}} \leftarrow$ **Local search** (S_{parent}, μ);
13	$S_{\text{parent}} \leftarrow$ **Nondominated sorting** (S_{parent});
14	$S_{\text{parent}} \leftarrow$ **Local sorting** (S_{parent}, γ, Z^0_{TTC}, Z^0_{PTT});
15	**While** $\lambda \leq \Lambda$ **do**
16	$S_{\text{elite}} \leftarrow$**Tournament selection** (S_{parent});
17	$S_{\text{offspring}} \leftarrow$**Crossover and mutation** (S_{elite}, P, P_π, $P_{\bar{\omega}}$);
18	$S_{\text{hybrid}} \leftarrow$**Population combination** (S_{parent}, $S_{\text{offspring}}$);
19	$S_{\text{hybrid}} \leftarrow$**Local search** ($S_{\text{hybrid}}$, μ);
20	$S_{\text{hybrid}} \leftarrow$**Nondominated sorting** (S_{hybrid});
21	$S_{\text{hybrid}} \leftarrow$**Local sorting** ($S_{\text{hybrid}}$, γ, Z^0_{TTC}, Z^0_{PTT});
22	$S_{\text{parent}} \leftarrow$**Population replacement** (S_{hybrid});
23	$S^\lambda_{\text{Pareto}} \leftarrow$**POSS extraction** ($S_{\text{parent}}$);
24	P, P_π, $P_{\bar{\omega}} \leftarrow$**Operator scoring** ($S_{\text{parent}}$, S_{hybrid}, Λ^0);
25	**If** $S^\lambda_{\text{Pareto}} = S^{\lambda-\Lambda}_{\text{Pareto}}$ **then**
26	**Break**;
27	**End if**
28	$\lambda \leftarrow \lambda + 1$;
29	**End while**
30	**Return** $S^\lambda_{\text{Pareto}}$;
31	**End**

4.2. Algorithm Improvements. We only focus on the improvements in NSCMA since AANSGA-II was introduced comprehensively in our previous work [22]. The improvements are reflected in chromosome construction, local search, and local sorting.

4.2.1. Improvements in Chromosome Construction. AANSGA-II encodes real variables h^l_k (i.e., headway of train k_l) instead of binary variables x^l_{kt} as genes to express the GA information. The chromosome in AANSGA-II is $(h^1_1, h^1_2, \cdots, h^1_K, h^2_1, h^2_2, \cdots, h^2_K, \cdots, h^L_1, h^L_2, \cdots, h^L_K)$.

Differing from AANSGA-II, NSCMA encodes integer variable n_1 and binary variables n_2, n_3, and n_4 as memes to express the LS settings. Integer variable n_1 represents the position (i.e., line) of LS, which is between 1 and L. Binary variable n_2 expresses the direction of LS. $n_2 = 0$ means to broad the headway, while $n_2 = 1$ means to narrow the headway. Binary variable n_3 represents the step of LS. $n_3 = 0$ means to move τ, while $n_3 = 1$ means to move 2τ. Binary variable n_4 expresses the strategy of LS. $n_4 = 0$ means overall movement, while $n_4 = 1$ means local movement. The chromosome in NSCMA is $(h^1_1, h^1_2, \cdots, h^1_K, h^2_1, h^2_2, \cdots, h^2_K, \cdots, h^L_1, h^L_2, \cdots, h^L_K, n_1, n_2, n_3, n_4)$, as illustrated in Figure 2.

As a module of the chromosome, the LS settings participate in crossover and mutation just like the GA information. In each crossover operation, the LS settings of the two individuals are partially exchanged. In each mutation operation, the LS settings of the individual are partially replaced.

4.2.2. Improvements in Local Search. AANSGA-II adopts all individuals in the hybrid population without processing. Due to the nature of crossover and mutation, the child population is generated without an optimization guarantee. The optimization mechanism in AANSGA-II is entirely nondeterministic.

Differing from AANSGA-II, NSCMA introduces LS to enhance the optimization guarantee. Several representative weights μ are preset to obtain all elite individuals in the first frontier since only elite individuals are valuable for decision makers. Each elite individual performs LS according to its LS settings. The processed individual is accepted if an improvement is achieved, and the original individual is retained otherwise. As the nature of LS, the processed population is optimized with an optimization guarantee. The optimization mechanism in NSCMA is partially deterministic.

4.2.3. Improvements in Local Sorting. AANSGA-II sequences all individuals in each frontier by local sorting. Local sorting is based on neighborhood distance. The individuals in AANSGA-II have descending original neighborhood distances.

Differing from AANSGA-II, NSCMA proposes a reference point to improve local sorting. The reference point is

Figure 2: Structure of chromosome.

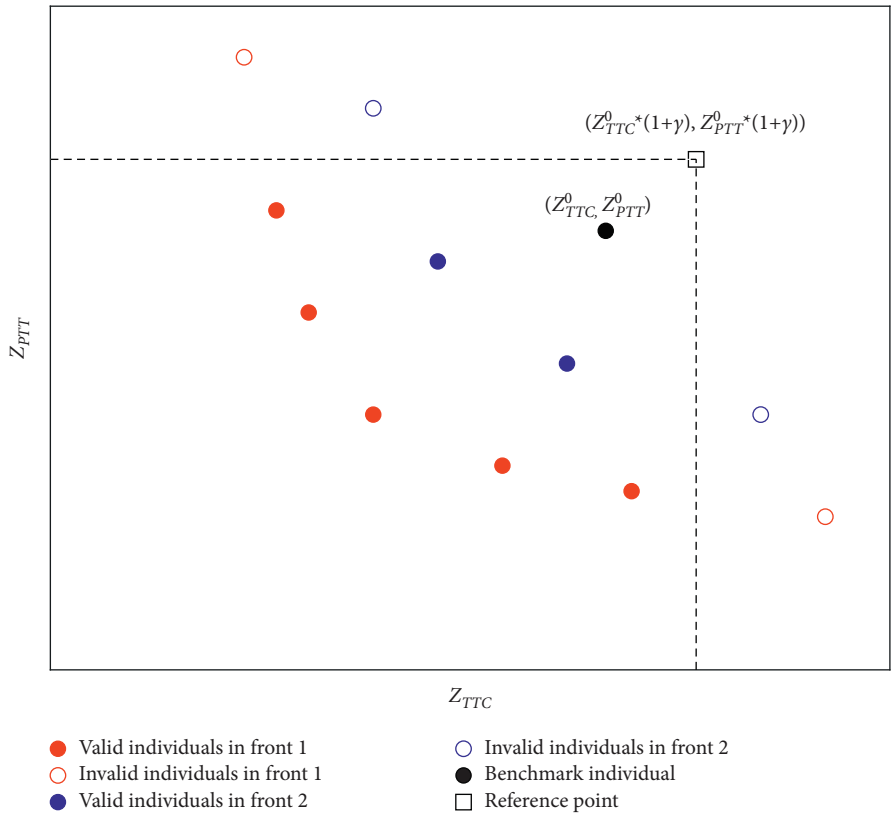

Figure 3: Classification of valid and invalid solutions.

composed of the maximum acceptable objective values for decision makers. An individual is valid if it dominates the reference point and invalid otherwise. On this basis, all individuals in each frontier are classified into valid individuals and invalid individuals. Since valid individuals are more valuable than invalid individuals, the neighborhood distances of valid individuals are retained, while the neighborhood distances of invalid individuals are cleared. The individuals in NSCMA have descending processed neighborhood distances.

Since the benchmark individual with trains' total cost Z^0_{TTC} and passengers' total time Z^0_{PTT} may be too excellent to serve as the reference point, NSCMA proposes tolerance factor γ to expend the maximum acceptable objective values to $Z^0_{TTC} * (1+\gamma)$ and $Z^0_{PTT} * (1+\gamma)$, as illustrated in Figure 3.

5. Case Study

5.1. Case Setup. Shenyang Metro in Northeast China operated a cruciform rail transit network from December 30, 2013, to April 7, 2018, as illustrated in Figure 4.

Dynamic passenger demand is strictly processed from the historical data on December 9, 2016. The distribution of passenger demand is bimodal, as illustrated in Figure 5.

The actual TOPs of the two lines are encoded together as the Benchmark Solution (BS for short). The time period of each line is normalized to [4 : 50, 22 : 20]. Table 2 demonstrates the parameters of the case.

The case focuses on the approximate POSS based on the STOPO model (SS for short) and the approximate POSS based on the ATOPO model (AS for short). Notably, AS of Line 1 (AS-1 for short) and AS of Line 2 (AS-2 for short) are optimized independently. Each solution in AS-1 and each solution in AS-2 form an integrated solution together. AS refers to the POSS in all integrated solutions.

The case applies NSCMA and AANSGA-II for comparisons. Both heuristic algorithms are encoded in MATLAB R2019a. All computations were performed on a personal computer. Table 3 demonstrates the parameters of the heuristic algorithms.

5.2. Case Results. Firstly, we solve the STOPO model with NSCMA and AANSGA-II. NSCMA obtains SS at generation 8491 within 123 min, while AANSGA-II obtains SS^* at

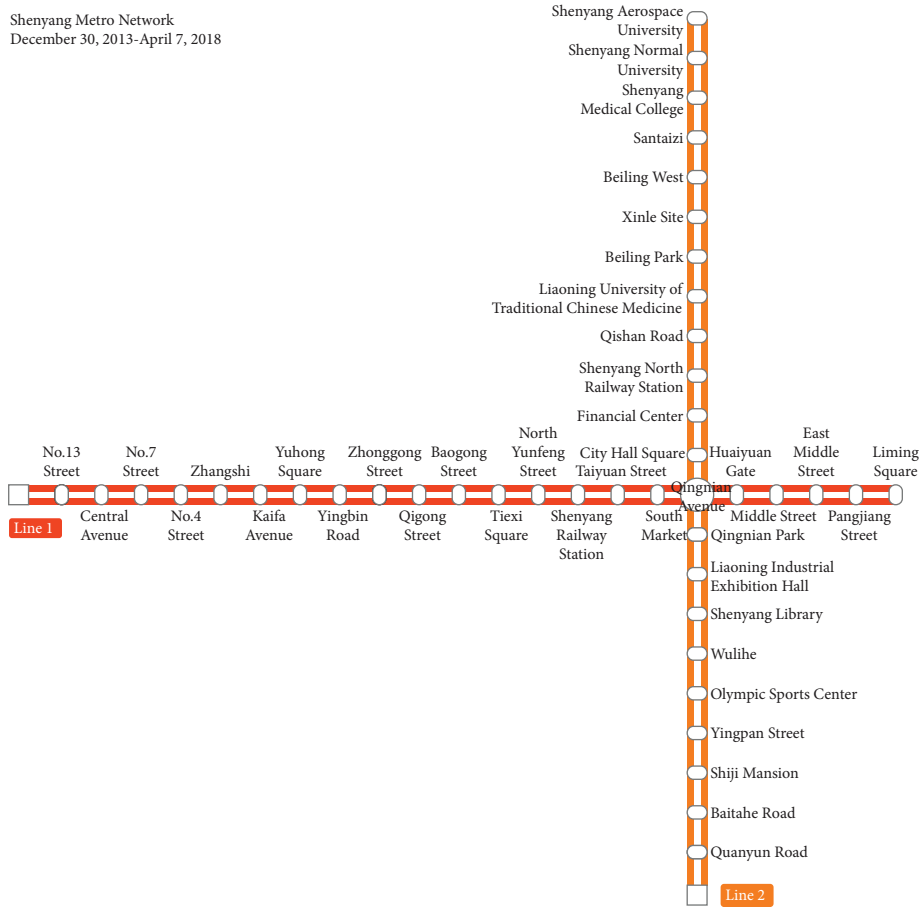

Figure 4: Sketch map of Shenyang Metro.

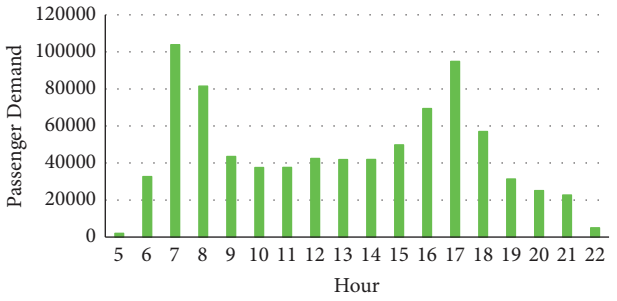

Figure 5: Distribution of passenger demand on December 9, 2016.

generation 9773 within 127 min. We use trains' total cost Z_{TTC} and passengers' total time Z_{PTT} as indicators to compare the performances of SS, SS*, and BS, as illustrated in Figure 6. Notably, only the solutions better than BS in both costs, also known as the valid solutions, are drawn in Figure 6.

According to Figure 6, SS outperforms SS* in progressiveness, while SS does not outperform SS* in diversity. SS dominates SS*, which means that NSCMA is better than AANSGA-II in the evolution process for the elite individuals. However, SS* presents more small cracks but fewer large cracks than SS, which means that NSCMA is not better than AANSGA-II in the evolution process for the first frontier.

Secondly, we solve the ATOPO model by NSCMA. NSCMA obtains AS-1 at generation 1142 within 7 min and AS-2 at generation 304 within 2 min. AS is selected from all combinations of AS-1 and AS-2 within 1 min. We use trains' total cost Z_{TTC} and passengers' total time Z_{PTT} as indicators to compare the performances of SS, AS, and BS, as illustrated in Figure 7.

In the light of Figure 7, SS contains thirty-four solutions, while AS contains fifteen solutions. SS dominates AS, obviously, which means that the STOPO model is better than the ATOPO model.

Thirdly, we list the Elite Solutions in SS (SS-Es for short) and the Elite Solutions in AS (AS-Es for short) under specific weights. Inspired by our previous work, the representative weights are $\mu \in \{0.05, 0.072, 0.1037, 0.1493, 0.215, 0.3096\}$ [22]. These six numbers form a proportional sequence with a common ratio of 1.44. We use trains' total cost Z_{TTC}, passengers' total time Z_{PTT}, generalized cost Z, and improvement rates over BS Δ_{TTC}, Δ_{PTT}, and Δ_Z as indicators to compare the performances of SS-Es, AS-Es, and BS under different μ, as demonstrated in Table 4. Notably, all elitist solutions are marked in Figure 7.

According to Table 4, both elite solution sets consist of five distinct solutions, respectively. Compared with BS, SS-Es improve Z_{TTC} by 4.35% and Z_{PTT} by 5.51% on average, while AS-Es improve Z_{TTC} by 1.57% and Z_{PTT} by 1.39% on

Table 2: Parameters of the case.

Parameter	Description	Value
L	The number of lines	2
I_l	The number of stations in each direction	22 (line 1, line 2), 44 (total)
J_l	The number of transfer stations in each direction	1 (line 1, line 2), 2 (total)
K_l^0	The minimum number of trains	153 (line 1), 136 (line 2), 289 (total)
K_l	The maximum number of trains	180 (line 1), 160 (line 2), 340 (total)
T_l^0	The start time of the time period	1 (line 1, line 2)
T_l	The end time of the time period	2100 (line 1, line 2)
c_l	The capacity of each train	2016 (line 1, line 2)
$h_{\min}^l$	The minimum headway of each train (min)	4 (line 1, line 2)
$h_{\max}^l$	The maximum headway of each train (min)	10 (line 1, line 2)
e_l^0	The essential cycle time of each connection (min)	112 (line 1), 111 (line 2)
τ	The length of each time slice (min)	0.5
m_l	The unit operation cost of each train (CNY)	852 (line 1), 834 (line 2)
m_l^0	The unit depreciation cost of each rolling stock (CNY)	3696 (line 1, line 2)
ε	The unit penalty time of each finally stranded passenger (min)	1000

Table 3: Parameters of the heuristic algorithms.

Parameter	Description	Value
Λ	The number of generations for final termination	10000
Λ'	The number of generations for early termination	50
Λ^0	The number of generations for operator scoring	50
Θ	The size of population	50 (SS), 20 (AS)
μ	The representative weights of passengers' total time	{0.05, 0.072, 0.1037, 0.1493, 0.215, 0.3096}
P	The initial probability of crossover operation	0.5
P_π	The initial probability of each crossover operator	0.5
P_ω	The initial probability of each mutation operator	0.0625
γ	The tolerance factor of reference point	0.03
Z_{TTC}^0	The trains' total cost of benchmark individual (CNY)	447552
Z_{PTT}^0	The passengers' total time of benchmark individual (min)	3163228.25

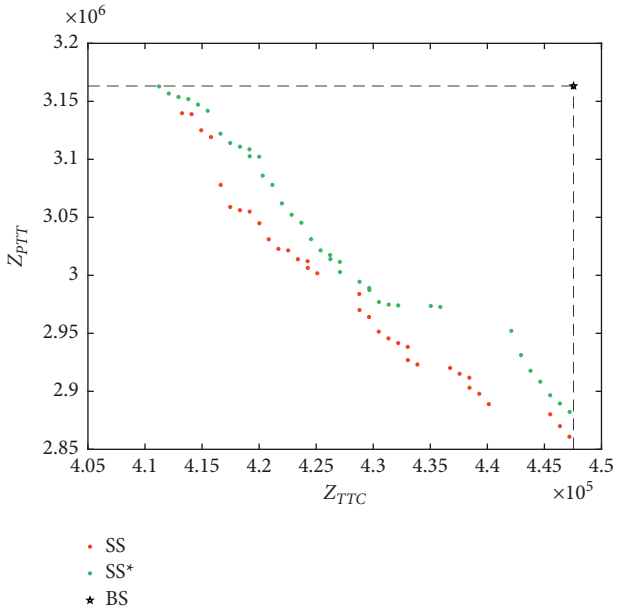

Figure 6: Performances of SS, SS^*, and BS.

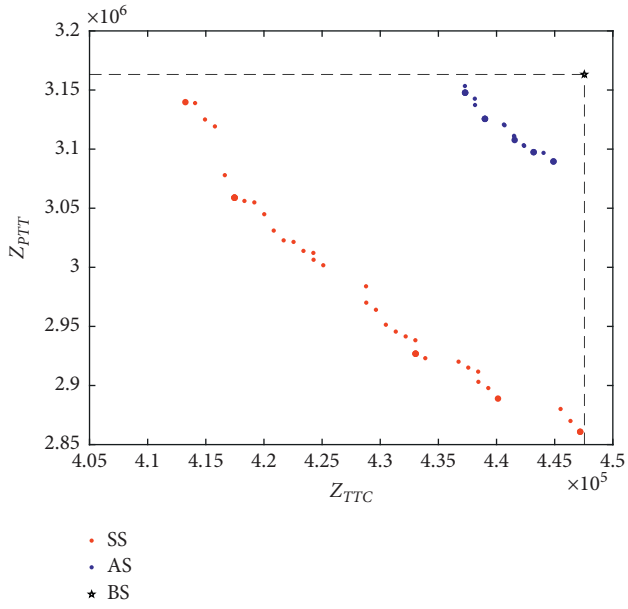

Figure 7: Performances of SS, AS, and BS.

Table 4: Performances of SS-Es, AS-Es and BS under different μ.

μ	Solution	Z_{TTC}	Δ_{TTC}	Z_{PTT}	Δ_{PTT}	Z	Δ_Z
0.05	SS-E-1	413244	7.67%	3139740.25	0.74%	570231.01	5.86%
	AS-E-1	437298	2.29%	3147741.75	0.49%	594685.09	1.82%
	BS	447552	—	3163228.25	—	605713.41	—
0.072	SS-E-2	417468	6.72%	3058919.75	3.30%	637710.22	5.57%
	AS-E-1	437298	2.29%	3147741.75	0.49%	663935.41	1.68%
	BS	447552	—	3163228.25	—	675304.43	—
0.1037	SS-E-2	417468	6.72%	3058919.75	3.30%	734616.80	5.27%
	AS-E-2	439002	1.91%	3125601.25	1.19%	763064.34	1.61%
	BS	447552	—	3163228.25	—	775515.50	—
0.1493	SS-E-3	433038	3.24%	2926909.25	7.47%	870023.21	5.41%
	AS-E-3	441558	1.34%	3107683.75	1.76%	905532.70	1.55%
	BS	447552	—	3163228.25	—	919819.45	—
0.215	SS-E-4	440124	1.66%	2888932.25	8.67%	1061217.99	5.89%
	AS-E-4	443190	0.97%	3097419.75	2.08%	1109106.90	1.64%
	BS	447552	—	3163228.25	—	1127617.12	—
0.3096	SS-E-5	447192	0.08%	2860860.25	9.56%	1332876.63	6.59%
	AS-E-5	444894	0.59%	3089543.75	2.33%	1401376.03	1.79%
	BS	447552	—	3163228.25	—	1426845.78	—
Average	SS-E	428089	4.35%	2989046.92	5.51%	867779.31	5.86%
	AS-E	440540	1.57%	3119288.67	1.39%	906283.41	1.68%
	BS	447552	—	3163228.25	—	921802.62	—

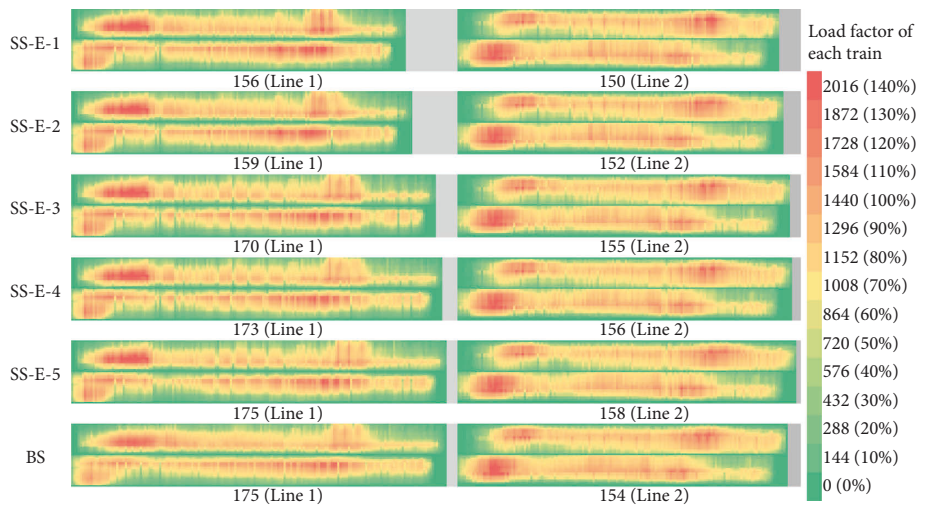

Figure 8: Utilization of trains in SS-Es and BS.

average. Compared with AS-Es, SS-Es improve Z_{TTC} by 2.83% and Z_{PTT} by 4.18% on average.

Fourthly, we use the load factor of each train as an indicator to analyze the utilization of trains in SS-Es and BS, as illustrated in Figure 8.

In the light of Figure 8, most SS-Es utilize trains more effectively than BS. Overall, SS-E-1 uses twenty-three fewer trains than BS, SS-E-2 uses eighteen fewer trains than BS, SS-E-3 uses four fewer trains than BS, SS-E-4 uses the same number of trains as BS, and SS-E-5 uses four more trains than BS. Specifically, no SS-E uses more trains on Line 1 than BS, while three SS-Es use more trains on Line 2 than BS. The difference demonstrates that the actual TOP of Line 1 has more space for optimization than that of Line 2. Besides, fewer trains generally mean higher average load factors.

Fifthly, we use the task order of each rolling stock as an indicator to analyze the utilization of rolling stocks in SS-Es and BS, as illustrated in Figure 9.

According to Figure 9, all SS-Es utilize rolling stocks more effectively than BS. Overall, SS-E-1 and SS-E-2 use four fewer rolling stocks than BS, SS-E-3 uses three fewer rolling stocks than BS, SS-E-4 uses two fewer rolling stocks than BS, and SS-E-5 uses one fewer rolling stocks than BS. Specifically, all SS-Es use fewer rolling stocks on Line 1 than BS, while no SS-E uses fewer rolling stocks on Line 2 than BS. The difference proves again that the actual TOP of Line 2 matches passenger demand better than that of Line 1.

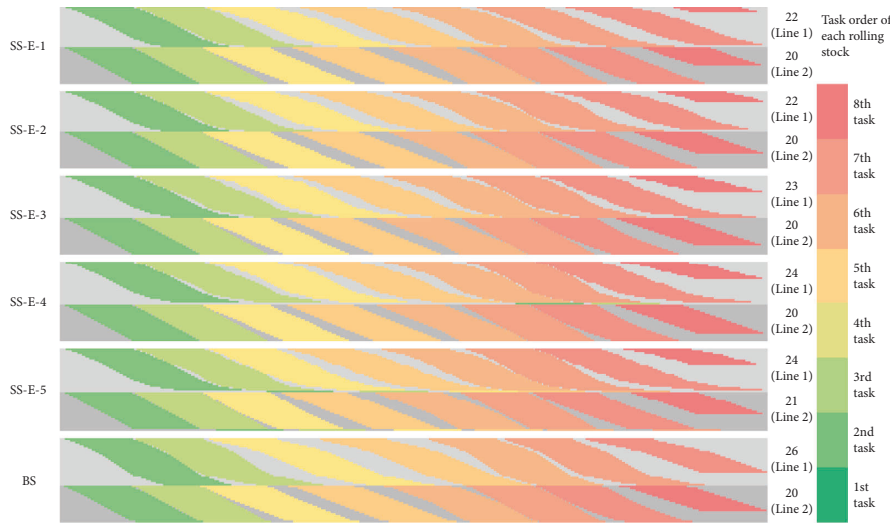

Figure 9: Utilization of rolling stocks in SS-Es and BS.

Besides, fewer rolling stocks generally mean more tasks per rolling stock.

In summary, the superiority of the STOPO model over the ATOPO model explains that TOPS is an important element in TOPO for the network. Besides, the superiority of NSCMA over AANSGA-II suggests that LS is a powerful complement to evolutionary algorithms.

6. Conclusion

This paper researched the demand-driven TOPO problem in the rail transit network. The bi-objective MILP models, the ATOPO model, and the STOPO model minimize trains' total cost and passengers' total time by simultaneously determining train frequency, train timetable, and rolling stock circulation. The hybrid heuristic algorithm, NSCMA, ameliorates the evolution process for elite individuals by incorporating CMA into AANSGA-II.

According to the case of Shenyang Metro, the STOPO model is better than the ATOPO model. The elite synchronous TOPs reduce trains' total cost by 2.83% and passengers' total time by 4.18% on average compared to the elite asynchronous TOPs. Besides, NSCMA is better than AANSGA-II. NSCMA outperforms AANSGA-II in obtaining the elite individuals, while NSCMA does not outperform AANSGA-II in obtaining the first frontier.

In the future, we will focus on the difficulties as follows. Firstly, the weight of passengers' total time is discussed with an alternative set. It is meaningful to integrate all objectives into a unified dimension. Secondly, NSCMA does not show comprehensive improvement over AANSGA-II. It is optional to apply other heuristic algorithms.

Data Availability

The passenger demand data used to support the findings of this study have not been made available because of the secrecy agreement.

Conflicts of Interest

The authors declare that they have no conflicts of interest.

Acknowledgments

This paper was supported by the National Natural Science Foundation of China (71971019), the Fundamental Research Funds for the Central Universities (2020JBZD007), the Frontiers Science Center for Smart High-Speed Railway System, and the Beijing Natural Science Foundation (L201013).

References

[1] Y. Yang, Z. Yuan, J. Chen, and M. Guo, "Assessment of osculating value method based on entropy weight to transportation energy conservation and emission reduction," *Environmental Engineering and Management Journal*, vol. 16, no. 10, pp. 2413–2423, 2017.

[2] H. Niu and X. Zhou, "Optimizing urban rail timetable under time-dependent demand and oversaturated conditions," *Transportation Research Part C: Emerging Technologies*, vol. 36, pp. 212–230, 2013.

[3] E. Barrena, D. Canca, L. C. Coelho, and G. Laporte, "Single-line rail rapid transit timetabling under dynamic passenger demand," *Transportation Research Part B: Methodological*, vol. 70, pp. 134–150, 2014.

[4] H. Niu, X. Zhou, and R. Gao, "Train scheduling for minimizing passenger waiting time with time-dependent demand and skip-stop patterns: nonlinear integer programming models with linear constraints," *Transportation Research Part B: Methodological*, vol. 76, pp. 117–135, 2015.

[5] T. Zhang, D. Li, and Y. Qiao, "Comprehensive optimization of urban rail transit timetable by minimizing total travel times under time-dependent passenger demand and congested conditions," *Applied Mathematical Modelling*, vol. 58, pp. 421–446, 2018.

[6] Y. Yin, D. Li, N. Bešinović, and Z. Cao, "Hybrid demand-driven and cyclic timetabling considering rolling stock circulation for a bidirectional Railway line," *Computer-Aided*

Civil and Infrastructure Engineering, vol. 34, no. 2, pp. 164–187, 2019.

[7] P. Mo, L. Yang, Y. Wang, and J. Qi, "A flexible Metro train scheduling approach to minimize energy cost and passenger waiting time," *Computers & Industrial Engineering*, vol. 132, pp. 412–432, 2019.

[8] S. Yang, F. Liao, J. Wu, H. J. P. Timmermans, H. Sun, and Z. Gao, "A Bi-objective timetable optimization model incorporating energy allocation and passenger assignment in an energy-regenerative Metro system," *Transportation Research Part B: Methodological*, vol. 133, pp. 85–113, 2020.

[9] X. Dong, D. Li, Y. Yin, S. Ding, and Z. Cao, "Integrated optimization of train stop planning and timetabling for commuter railways with an extended adaptive large neighborhood search metaheuristic approach," *Transportation Research Part C: Emerging Technologies*, vol. 117, p. 102681, 2020.

[10] Z. Cao, A. A. Ceder, D. Li, and S. Zhang, "Robust and optimized urban rail timetabling using a marshaling plan and skip-stop operation," *Transportmetrica: Transportation Science*, vol. 16, no. 3, pp. 1217–1249, 2020.

[11] R. Yang, B. Han, Q. Zhang, Z. Han, and Y. Long, "Integrated optimization of train route plan and timetable with dynamic demand for the urban rail transit line," *Transportation Business: Transport Dynamics*, vol. 26, pp. 1–34, 2022.

[12] R. C. W. Wong, T. W. Y. Yuen, K. W. Fung, and J. M. Y. Leung, "Optimizing timetable synchronization for rail mass transit," *Transportation Science*, vol. 42, no. 1, pp. 57–69, 2008.

[13] J. Wu, M. Liu, H. Sun, T. Li, Z. Gao, and D. Z. W. Wang, "Equity-based timetable synchronization optimization in urban subway network," *Transportation Research Part C: Emerging Technologies*, vol. 51, pp. 1–18, 2015.

[14] X. Guo, H. Sun, J. Wu, J. Jin, J. Zhou, and Z. Gao, "Multi-period-based timetable optimization for Metro transit networks," *Transportation Research Part B: Methodological*, vol. 96, pp. 46–67, 2017.

[15] X. Liu, M. Huang, H. Qu, and S. Chien, "Minimizing Metro transfer waiting time with AFCS data using simulated annealing with parallel computing," *Journal of Advanced Transportation*, vol. 75, pp. 1–17, 2018.

[16] X. Tian and H. Niu, "A Bi-objective model with sequential search algorithm for optimizing network-wide train timetables," *Computers & Industrial Engineering*, vol. 127, pp. 1259–1272, 2019.

[17] Z. Cao, A. A. Ceder, D. Li, and S. Zhang, "Optimal synchronization and coordination of actual passenger-rail timetables," *Journal of Intelligent Transportation Systems*, vol. 23, no. 3, pp. 231–249, 2019.

[18] H. Niu, X. Tian, and X. S. Zhou, "Demand-driven train schedule synchronization for high-speed rail lines," *IEEE Transactions on Intelligent Transportation Systems*, vol. 16, no. 5, pp. 2642–2652, 2015.

[19] T. Robenek, Y. Maknoon, S. S. Azadeh, J. Chen, and M. Bierlaire, "Passenger centric train timetabling problem," *Transportation Research Part B: Methodological*, vol. 89, pp. 107–126, Jul 2016.

[20] P. Shang, R. Li, Z. Liu, K. Xian, and J. Guo, "Timetable synchronization and optimization considering time-dependent passenger demand in an urban subway network," *Transportation Research Record Journal of the Transportation Research Board*, vol. 2672, no. 8, pp. 243–254, 2018.

[21] Y. Wang, D. Li, and Z. Cao, "Integrated timetable synchronization optimization with capacity constraint under time-dependent demand for a rail transit network," *Computers & Industrial Engineering*, vol. 142, p. 106374.

[22] Z. Han, B. Han, D. Li, S. Ning, R. Yang, and Y. Yin, "Train timetabling in rail transit network under uncertain and dynamic demand using advanced and adaptive NSGA-II," *Transportation Research Part B: Methodological*, vol. 154, pp. 65–99, 2021.

[23] Z. Yao, H. Jiang, Y. Cheng, Y. Jiang, and B. Ran, "Integrated schedule and trajectory optimization for connected automated vehicles in a conflict zone," *IEEE Transactions on Intelligent Transportation Systems*, vol. 23, no. 3, pp. 1841–1851, 2022.

[24] C. S. Ying, A. H. F. Chow, and K. S. Chin, "An actor-critic deep reinforcement learning approach for Metro train scheduling with rolling stock circulation under stochastic demand," *Transportation Research Part B: Methodological*, vol. 140, pp. 210–235, 2020.

[25] Y. Yang, K. He, Y. p. Wang, Z. z. Yuan, Y. h. Yin, and M. z. Guo, "Identification of dynamic traffic crash risk for cross-area freeways based on statistical and machine learning methods," *Physica A: Statistical Mechanics and Its Applications*, vol. 595, p. 127083.

[26] Y. Yang, Z. Yuan, and R. Meng, "Exploring traffic crash occurrence mechanism toward cross-area freeways via an improved data mining approach," *Journal of Transportation Engineering Part A: Systems*, vol. 148, no. 9, 2022.

[27] X. Cai and C. J. Goh, "A fast heuristic for the train scheduling problem," *Computers & Operations Research*, vol. 21, no. 5, pp. 499–510, 1994.

[28] K. Deb, A. Pratap, S. Agarwal, and T. Meyarivan, "A fast and elitist multiobjective genetic algorithm: nsga-II," *IEEE Transactions on Evolutionary Computation*, vol. 6, no. 2, pp. 182–197, 2002.

[29] H. Wang, D. Wang, and S. Yang, "A memetic algorithm with adaptive hill climbing strategy for dynamic optimization problems," *Soft Computing*, vol. 13, no. 8-9, pp. 763–780, 2008.

[30] D. Tang, Z. Liu, J. Yang, and J. Zhao, "Memetic frog leaping algorithm for global optimization," *Soft Computing*, vol. 23, no. 21, pp. 11077–11105, 2018.

[31] J. E. Smith, "Co-evolving memetic algorithms: a learning approach to robust scalable optimisation," in *Proceedings of the IEEE Congress on Evolutionary Computation*, pp. 498–505, Canberra, AUSTRALIA, 2003.

[32] E. Özcan, J. H. Drake, C. Altıntaş, and S. Asta, "A self-adaptive multimeme memetic algorithm Co-evolving utility scores to control genetic operators and their parameter settings," *Applied Soft Computing*, vol. 49, pp. 81–93, 2016.

[33] M. Frutos, A. C. Olivera, and F. Tohmé, "A memetic algorithm based on a NSGAII scheme for the flexible job-shop scheduling problem," *Annals of Operations Research*, vol. 181, no. 1, pp. 745–765, 2010.

[34] C. Cobos, C. Erazo, and J. Luna, "Multi-objective memetic algorithm based on NSGA-II and simulated annealing for calibrating CORSIM micro-simulation models of vehicular traffic flow," *Advances in Artificial Intelligence*, vol. 43, pp. 468–476, 2016.